The generalized resonating valence bond description of cyclobutadiene

ARTICLE *in* JOURNAL OF THE AMERICAN CHEMICAL SOCIETY · MAY 1986

Impact Factor: 12.11 · DOI: 10.1021/ja00271a008

2 AUTHORS, INCLUDING:

William A. Goddard
California Institute of Technology
1,323 PUBLICATIONS **67,032** CITATIONS

Higginson and Marshall[20] determined that reaction 7 becomes important at pHs higher than 5. As the pH is increased this process becomes faster and more complete. The ferricyanide oxidation of the sulfite results in a lag period in the oscillation. The sulfite cannot build up to a level where the Landolt reaction can resume, point I, until the ferricyanide is either reduced back to ferrocyanide or is washed out of the reactor.

In general, the oscillation begins with the Landolt reaction. The ferrocyanide does not disturb the reaction, since it reacts much more slowly with the iodate than does the sulfite. The Landolt reaction proceeds until all the sulfite has been consumed. At this point the $Fe(CN)_6^{4-}$ comes into the picture as it reacts with the I_2 formed in the Landolt reaction. The product of this reaction, $Fe(CN)_6^{3-}$, serves as an inhibitor to the Landolt reaction. Only after the ferricyanide is removed can the oscillation begin again. Thus the ferrocyanide–ferricyanide redox couple serves two purposes. First, by reacting with the I_2 it permits the system to return to SSI. Second, by slowing down the sulfite buildup the ferricyanide creates a time lag which results in oscillatory rather than steady-state behavior. It is necessary that the temperature be high enough so that this reaction can take place sufficiently rapidly.

The discovery of the iodate–sulfite–ferrocyanide oscillator is of significance to the study of chemical oscillations for several reasons. It provides an almost classic example of the utility of the cross shaped phase diagram approach[11,12] in searching for new oscillators. It suggests that the family of iodate oscillators may well be comparable in size to the other oxyhalogen families, though the search may have to be carried out above room temperature.

Finally, this system seems ideal for both dynamical and mechanistic studies. In addition to the pH and redox probes on which we have focused in this report, it is possible to measure $[I^-]$ potentiometrically and $[I_2]$, $[Fe(CN)_6^{4-}]$, and $[Fe(CN)_6^{3-}]$ spectrophotometrically. Such data would facilitate both the generation of multidimensional phase portraits and the development and testing of detailed mechanisms. Studies are now under way in our laboratories to determine several of the relevant rate constants so that the mechanistic suggestions sketched above can be converted to a full mechanism for this fascinating system.

Acknowledgment. This work was supported by a U.S.–Hungarian Cooperative Grant from the National Science Foundation (INT8217658 and CHE8419949) and the Hungarian Academy of Sciences.

The Generalized Resonating Valence Bond Description of Cyclobutadiene

Arthur F. Voter[†] and William A. Goddard, III*

Contribution No. 7151 from the Arthur Amos Noyes Laboratory of Chemical Physics, California Institute of Technology, Pasadena, California 91125. *Received February 13, 1985*

Abstract: The low-lying electronic states of square and rectangular cyclobutadiene (CBD) are calculated by using the generalized resonating valence bond (GRVB) method and compared with the results from Hartree–Fock and configuration interaction wavefunctions. We find that simple valence bond concepts correctly predict the sequence of excited states (including ground-state singlet) and the distortion to a rectangular geometry for the ground state. Contrary to common expectation, we find that the singlet ground state of square CBD has 22 kcal of resonance energy (relative to a single valence bond structure). Thus, CBD is *not* antiresonant, though it is much less stable than normal conjugated systems.

I. Introduction

Cyclobutadiene (CBD), the simplest cyclic four-electron π system, has provided an interesting counterpoint to benzene for many years. In agreement with simple Hückel theory arguments, the molecule is highly unstable, though it has been isolated in low-temperature matrix studies[1] and observed as a short-lived intermediate in solution.[2,3] Two features of CBD are particularly intriguing. First, the most stable geometry is found to be rectangular (both experimentally[1-3] and theoretically[4-7]), with the square geometry (6–12 kcal higher) representing a saddle point for interconversion of the two rectangular structures.[8] Second, the lowest state at the square geometry is found to be a singlet, in contradiction to the prediction of a triplet ground state from molecular orbital (MO) theory.

The resonating valence bond (VB) model offers a useful alternative view of CBD, providing a simple rationalization of spin state and geometry; the CBD molecule thus provides a good vehicle for contrasting the VB and MO theories. In the following we discuss the electronic structure of square cyclobutadiene at a qualitative level from both points of view. We then quantify these arguments by using the orbitally-optimized generalizations of MO and VB theory and compare these results with accurate configuration interaction (CI) calculations. Finally, we consider distortions from the square geometry to give the observed rectangular geometry.

The orbitally-optimized representation of MO theory is simply the Hartree–Fock (HF) wave function, while for VB theory it is the generalized valence bond[9] (GVB) wave function. Because the resonance of more than one VB wave function is important for CBD, we will also apply the recently developed resonating GVB (R-GVB) method[10] in which two (or more) GVB wave functions are mixed, leading to a resonance-stabilized state and one or more antiresonant states. The true generalization of resonating-VB theory is the generalized resonating valence bond (GRVB) wave function[11] in which the GVB subwave functions are allowed to

[†] Present address: Theoretical Division, MS J569, Los Alamos National Laboratory, Los Alamos, NM 87545

(1) Masamune, S.; Souto-Bachiller, F. A.; Machiguchi, T.; Bertie, J. E. *J. Am. Chem. Soc.* **1978**, *100*, 4889.
(2) Whitman, D. W.; Carpenter, B. K. *J. Am. Chem. Soc.* **1980**, *102*, 4272.
(3) Whitman, D. W.; Carpenter, B. K. *J. Am. Chem. Soc.* **1982**, *104*, 6473.
(4) Kollmar, H.; Staemmler, V. *J. Am. Chem. Soc.* **1978**, *100*, 4304.
(5) Borden, W. T.; Davidson, E. R.; Hart, P. *J. Am. Chem. Soc.* **1978**, *100*, 388.
(6) Jafri, J. A.; Newton, M. D. *J. Am. Chem. Soc.* **1978**, *100*, 5012.
(7) Borden, W. T.; Davidson, E. R. *Acc. Chem. Res.* **1981**, *14*, 69.
(8) This was long a subject of controversy, since experimental evidence previously indicated a square geometry; see ref 2 and citations therein.
(9) Bobrowicz, F. W.; Goddard, W. A., III. In *Modern Theoretical Chemistry, Methods of Electronic Structure Theory*; Schaefer, H. F., III, Ed.; Plenum: New York, 1977; Vol. 3, Chapter 4.
(10) Voter, A. F.; Goddard, W. A., III. *J. Chem. Phys.* **1981**, *57*, 253.

0002-7863/86/1508-2830$01.50/0

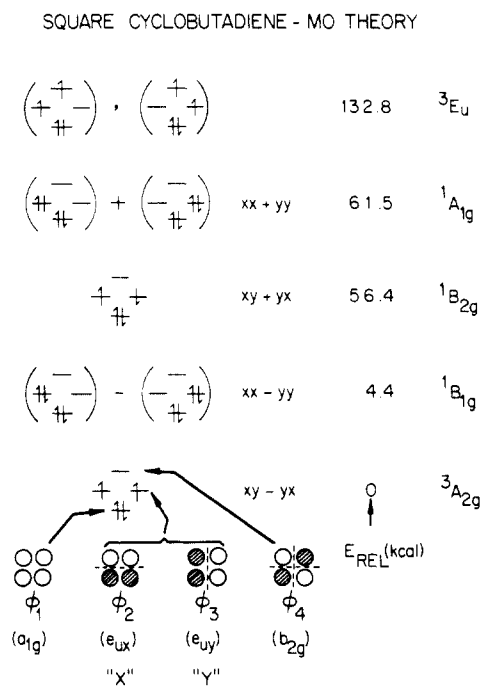

Figure 1. The MO theory description of the low-lying states of square cyclobutadiene. The energies are from separate HF calculations on each state.

optimize in the presence of the resonance. The distinctive feature of both the R-GVB and GRVB methods is that the GVB orbitals of different resonance configurations are allowed arbitrary overlap, thus retaining a faithful representation of the resonating-VB concept.

II. Molecular Orbital (MO) Approach—Square Geometry

In the MO wave function for CBD, one combines the four atomic π functions into four symmetry-adapted MO's, as shown in the bottom of Figure 1. Since φ_2 and φ_3 are degenerate, the ground state is $^3A_{2g}$

$$\Psi^{MO}(^3A_{2g}) = A[(\sigma \text{ core})\varphi_1^2\varphi_2\varphi_3\alpha\beta\alpha\alpha] \quad (1)$$

Considering all states involving two electrons distributed among the φ_2 and φ_3 orbitals leads to

$$\Psi^{MO}(^3A_{2g}) = (\varphi_2\varphi_3 - \varphi_3\varphi_2)(\alpha\beta + \beta\alpha) \quad (2a)$$

$$\Psi^{MO}(^1B_{2g}) = (\varphi_2\varphi_3 + \varphi_3\varphi_2)(\alpha\beta - \beta\alpha) \quad (2b)$$

$$\Psi^{MO}(^1B_{1g}) = (\varphi_2^2 - \varphi_3^2)(\alpha\beta - \beta\alpha) \quad (2c)$$

$$\Psi^{MO}(^1A_{1g}) = (\varphi_2^2 + \varphi_3^2)(\alpha\beta - \beta\alpha) \quad (2d)$$

(omitting the σ core and φ_1 orbitals common to all states and ignoring normalization). Factoring away the spin function, and replacing φ_2 by "X" and φ_3 by "Y" to denote their symmetry, leads to

$$^3A_{2g} = XY - YX \quad (3a)$$

$$^1B_{2g} = XY + YX \quad (3b)$$

$$^1B_{1g} = XX - YY \quad (3c)$$

$$^1A_{1g} = XX + YY \quad (3d)$$

Taking the orbital shapes to be the same for each state, the energies are

$$E(XY - YX) = E_0 + J_{XY} - K_{XY} \quad (4a)$$

$$E(XY + YX) = E_0 + J_{XY} + K_{XY} \quad (4b)$$

$$E(XX - YY) = E_0 + J_{XX} - K_{XY} \quad (4c)$$

$$E(XX + YY) = E_0 + J_{XX} + K_{XY} \quad (4d)$$

where J and K are the usual two-electron Coulomb and exchange integrals,

$$J_{XY} = \left\langle X(1)Y(2)\left|\frac{1}{r_{12}}\right|X(1)Y(2)\right\rangle \quad (5a)$$

$$K_{XY} = \left\langle X(1)Y(2)\left|\frac{1}{r_{12}}\right|Y(1)X(2)\right\rangle \quad (5b)$$

Since the J and K integrals are always positive, the MO analysis immediately shows that $E(XY - YX)$ lies below $E(XY + YX)$ and $E(XX - YY)$ lies below $E(XX + YY)$. Also, since J_{XX} must be greater than J_{XY} (two electrons have larger repulsion when in the same orbital), $E(XY - YX)$ is below $E(XX - YY)$ and $E(XY + YX)$ is below $E(XX + YY)$. Thus the $^3A_{2g}(XY - YX)$ state lies lowest, and the $^1A_{1g}(XX + YY)$ state lies highest, but we have not yet placed the $^1B_{2g}(XY + YX)$ and $^1B_{1g}(XX - YY)$ states relative to each other. To compare these, we make use of the fact that

$$XX - YY = \tfrac{1}{2}[(X + Y)(X - Y) + (X - Y)(X + Y)] \quad (6)$$

i.e., the XX - YY wave function is equivalent to singlet-coupling one electron in an X + Y orbital to one electron in an X - Y orbital. Thus E(XX - YY) becomes

$$E(XX - YY) = E_0 + J_{X+Y,X-Y} + K_{X+Y,X-Y} \quad (7)$$

From the shapes of the X + Y and X - Y orbitals,

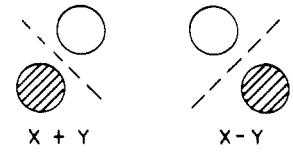

(8)

we see that the node in the X + Y orbital passes through the maximum density region of the X - Y orbital and vice versa, a result that is not true for the X and Y orbitals. Thus $J_{X+Y,X-Y}$ and $K_{X+Y,X-Y}$ are smaller than J_{XY} and K_{XY}, respectively, and $^1B_{1g}(XX - YY)$ is expected to lie below $^1B_{2g}(XY + YX)$. This qualitative MO state ordering is shown in Figure 1, along with the relative energies from HF calculations on each state. Even though HF allows different orbital shapes for each state, the ordering is exactly as predicted.

The $^1B_{1g}(XX - YY)$ state is only 4.4 kcal above the $^3A_{2g}(XY - YX)$ state. To compare these states, it is convenient to write both in terms of the X + Y and X - Y orbitals (8). This leads to (6) for $^1B_{1g}$ and

$$(XY - YX) = \tfrac{1}{2}[(X - Y)(X + Y) - (X + Y)(X - Y)] \quad (9)$$

for $^3A_{2g}$. Thus the energies of $^3A_{2g}$ and $^1B_{1g}$

$$E(^3A_{2g}) = E_0 + J_{X+Y,X-Y} - K_{X+Y,X-Y} \quad (10a)$$

$$E(^1B_{1g}) = E_0 + J_{X+Y,X-Y} + K_{X+Y,X-Y} \quad (10b)$$

differ by $2K_{X+Y,X-Y}$ so that

$$K_{X+Y,X-Y} \approx 2.2 \text{ kcal} \quad (11)$$

In contrast, using (4) to compare the $^1B_{2g}(XY + YX)$ state with the $^3A_{2g}(XY - YX)$ state yields

$$K_{XY} = 28.2 \text{ kcal} \quad (12)$$

so that K_{XY} is much larger than $K_{X+Y,X-Y}$, as expected. Thus, in MO theory, the lowest two states of CBD can be thought of as arising from the singlet and triplet couplings of the two weakly interacting orthogonal orbitals shown in (8).

We have also included in Figure 1 the first excited triplet state,

$$\Psi(^3E_u) = A[\varphi_1^2\varphi_2\varphi_4\alpha\beta\alpha\alpha] \quad (13)$$

which is seen to be far above the three singlets.

III. Resonating Valence Bond Approach—Square Geometry

In the valence bond (VB) formalism, the natural description of cyclobutadiene has two π bonds

(11) Voter, A. F.; Goddard, W. A., III. *J. Chem. Phys.* **1981**, *75*, 3638.

(14)

Denoting the atomic orbitals as a, b, c and d,

(15)

the wavefunction for the state with two π bonds can be taken as

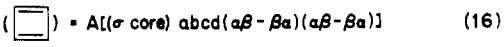

$$\Psi(\square) = A[(\sigma\ \text{core})\,abcd(\alpha\beta-\beta\alpha)(\alpha\beta-\beta\alpha)] \quad (16)$$

or as

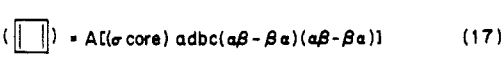

$$\Psi(\square) = A[(\sigma\ \text{core})\,adbc(\alpha\beta-\beta\alpha)(\alpha\beta-\beta\alpha)] \quad (17)$$

These two wavefunctions have equivalent energies, and the optimum description of the ground state is a resonance of these two wavefunctions,

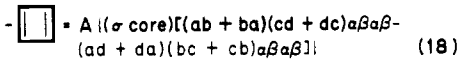

$$\Psi^{\text{R-VB}}(^1B_{1g}) = \square - \square = A\{(\sigma\ \text{core})[(ab+ba)(cd+dc)\alpha\beta\alpha\beta - (ad+da)(bc+cb)\alpha\beta\alpha\beta]\} \quad (18)$$

The other combination of (16) and 17)

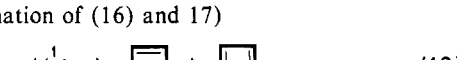

$$\Psi(^1A_{1g}) = \square + \square \quad (19)$$

leads to destabilization (the antiresonant state). To construct a triplet state, we must break one of these two π bonds, leading to four equivalent structures,

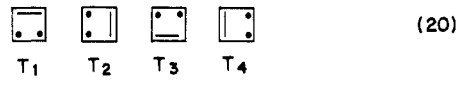

(20)

which can be written as

$$\Psi^{VB}(T_1) = A[(\sigma\ \text{core})abcd(\alpha\beta-\beta\alpha)\alpha\alpha] \quad (21a)$$

$$\Psi^{VB}(T_2) = A[(\sigma\ \text{core})bcda(\alpha\beta-\beta\alpha)\alpha\alpha] \quad (21b)$$

$$\Psi^{VB}(T_3) = A[(\sigma\ \text{core})cdab(\alpha\beta-\beta\alpha)\alpha\alpha] \quad (21c)$$

$$\Psi^{VB}(T_4) = A[(\sigma\ \text{core})dabc(\alpha\beta-\beta\alpha)\alpha\alpha] \quad (21d)$$

Combining these triplets into symmetry adapted wave functions leads to a resonant $^3A_{2g}$ state

$$\Psi^{R-VB}(^3A_{2g}) = T_1 + T_2 + T_3 + T_4 \quad (22)$$

and a degenerate pair of antiresonant states

$$\Psi^{R-VB}(^3E_u) = T_1 - T_3,\ T_2 - T_4 \quad (23)$$

(There are only three linearly independent triplets for four electrons in four orbitals,[12] so there is no fourth combination.) So far we have predicted four states, a resonant and antiresonant pair of singlets, and a resonant and antiresonant pair of triplets. Unless the resonance energy is much greater for the triplet state than for the singlet, we expect a ground state singlet and a low lying triplet.

In Figure 2 we show the splitting of the VB singlet and triplet wave functions into resonant and antiresonant states. The energies assigned to each state are the results of GVB and GRVB calculations, which find the best orbital shapes for the particular form of the wave function (VB or resonating VB). These resonating wave functions will be discussed in depth in the following sections.

Comparing the MO and VB wave functions, we see that both account for low-lying $^3A_{2g}$ and $^1B_{1g}$ state but that *VB puts* $^1B_{1g}$ *lower, whereas MO puts* $^3A_{2g}$ *lower*. In VB theory, the antiresonance combinations lead to high lying $^1A_{1g}$ and ^3E_u states, whereas in MO theory the third state is $^1B_{2g}$. To describe the $^1B_{2g}$ state in VB theory requires ionic configurations having two electrons in a single p orbital on one atom. For example,

$$\Psi^{R-VB}(^1B_{2g}) = A[(\sigma\ \text{core})\Phi\alpha\beta\alpha\beta] \quad (24)$$

(12) Pilar, F. L. *Elementary equantum Chemistry*; McGraw-Hill: New York, 1968; p 288.

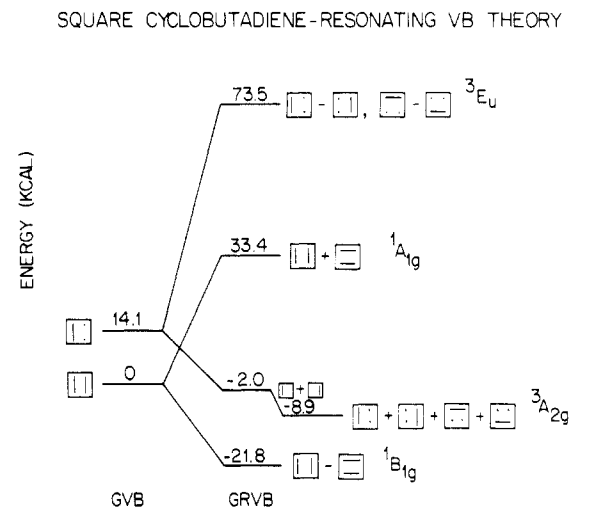

Figure 2. The resonating VB theory description of the low-lying states of square cyclobutadiene.

where Φ = aa(bd + db) + cc(bd + db) − bb(ac + ca) − dd(ac + ca).

IV. Calculational Details

All calculations employed the Dunning valence double-ζ contraction[13] of Huzinaga's 9s5p carbon basis[14] and the 4s hydrogen basis (scaled by 1.2). The square geometry was that optimized by Borden et al[5] (R_{CC} = 1.453, R_{CH} = 1.10). The rectangular calculation was performed at R_1 = 1.54 Å, R_2 = 1.38 Å, and R_{CH} = 1.10 Å, very near the geometry optimized by Walkup, Ho, and Goddard[15] for the singlet state by using a full π CI wave function in the same basis as ours. The HF wave functions used to describe the MO states were optimized by using the Caltech GVB2P5 program.[9] The triplet states were simple Hartree-Fock wave functions, while the singlet states were two configuration wave functions, as given by (2b), (2c), and (2d). The VB wave functions were also optimized with GVB2P5. The resonating VB wave functions were optimized by using the GRVB program,[11] while the R-GVB energies were evaluated by using the RESGVB program.[10] All GRVB and full π CI calculations were performed by using a frozen symmetric σ core taken from the $^1B_{2g}$ HF wave function for the square geometry and from the GVB(2/4) singlet for the rectangular geometry. With the σ core removed, the GRVB and CI calculations were optimized in a space of eight basis functions. The effect of allowing the σ space to relax was found to be only 1.2 kcal for the GVB(2/4) singlet state, so that use of a fixed σ core should have a negligible effect on the relative energies of various states.

The form of the GRVB(2/4) wave functions are not exactly as written in (18), since the orbitals are allowed to have a different shape in each resonance structure. Thus

$$\Psi^{GRVB}(^1B_{1g}) = A[(ab+ba)(cd+dc)\alpha\beta\alpha\beta - (a'd'+d'a')(b'c'+c'b')\alpha\beta\alpha\beta] \quad (25a)$$

$$\Psi^{GRVB}(^1A_{1g}) = A[(ab+ba)(cd+dc)\alpha\beta\alpha\beta + (a'd'+d'a')(b'c'+c'b')\alpha\beta\alpha\beta] \quad (25b)$$

and the result is that each orbital polarizes to achieve higher overlap with its bonding partner. We know that

$$\Psi(\square)$$

(13) Dunning, T. H., Jr.; Hay, P. J. In *Modern Theoretical Chemistry, Methods of Electronic Structure Theory*; Schaefer, H. F., III, Ed.; Plenum: New York, 1977; Vol. 3, Chapter 1.

(14) Huzinaga, S. *J. Chem. Phys.* **1965**, *42*, 1293.

(15) Walkup, R. E.; Ho, W.; Goddard, W. A., III, unpublished results. See: Ho, W. Senior Thesis, California Institute of Technology, 1975.

should be the 90° rotation of

$\psi($  $)$

and thus the primed set of orbitals is simply related to the unprimed set by

$$a = \hat{R}(b') \tag{26a}$$

$$b = \hat{R}(c') \tag{26b}$$

$$c = \hat{R}(d') \tag{26c}$$

$$d = \hat{R}(a') \tag{26d}$$

where $\hat{R}$ is the C_4 rotation operator. It is the wave functions given by (25) and (26) that are optimized, where separate GRVB calculations were performed for each state, leading to slightly different orbital shapes. The effect on the energy of allowing the orbitals to relax from GVB to GRVB is discussed in section VI. Since the orbitals of the second resonance structure are completely defined by the four orbitals of the first structure (related by the 90° rotation), the GRVB program utilizes just the four (natural) orbitals of one resonance structure.

For the GRVB(2/4) singlet state, D_{4h} symmetry could be used to reduce the calculation to a single unique π orbital, say φ_a, as indicated in (27)

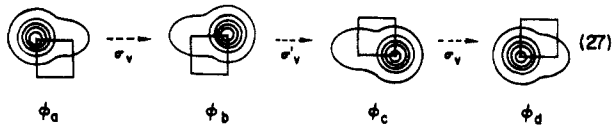

(27)

Since there are eight basis functions total, optimizing the shape of this one orbital would require optimizing only seven orbital rotations. However, this approach is cumbersome, since a general rotation of φ_a wiith one of the seven virtual orbitals would introduce an overlap between φ_a with φ_c and φ_d,[16] which is unallowed in the perfect pairing GVB wave function. Thus, after each orbital rotation, a symmetric orthogonalization would be necessary, to maintain both the required orthogonality and the symmetry relation between the orbitals. We instead optimize all four orbitals, in terms of the natural orbitals

$$\varphi_1 = \varphi_a + \varphi_b \tag{28a}$$

$$\varphi_2 = \varphi_a - \varphi_b \tag{28b}$$

$$\varphi_3 = \varphi_c + \varphi_d \tag{28c}$$

$$\varphi_4 = \varphi_c - \varphi_d \tag{28d}$$

and take advantage of the symmetry with respect to the σ_v reflection plane. Thus, there are two symmetric occupied orbitals (φ_1 and φ_3) that can mix with each other and with two symmetric virtual orbitals. In addition, there are two antisymmetric occupied orbitals (φ_2 and φ_4) that can mix with each other and with two virtuals, leading to a total of ten orbital rotations (five rotations per symmetry type).

The GRVB($^1/_2$) triplet wave function ($^3A_{2g}$) was optimized by (i) optimizing the orbitals by using only two of the four resonance structures shown in (22) (T_1 and T_3) and then (ii) using the RESGVB program[10] to rotate these orbitals and to construct the full four-structure resonating wavefunction (22). The effect of including the two extra resonance structures is seen from Figure 2 to be 6.9 kcal, but the effect of *optimizing* the orbitals with four structures rather than two is expected to be negligible. This is because the dominant effect in going from GVB to GRVB is the localization of the orbitals, which is already complete for the two-configuration wave function (Figure 5). It is interesting to note that if the orbital shapes a, b, c, and d are restricted to be the same for each resonance structure, as written in the VB wave functions (19a)–(19d), then the two-structure form of the triplet is equivalent to the four-structure form, since

$$T_1 + T_3 = T_2 + T_4 \tag{29}$$

The 6.9 kcal lowering we observe by including the third and fourth structures indicates the importance of allowing the orbitals to polarize for optimum bonding overlap.

Simultaneously optimizing four symmetry-related structures for $^3A_{2g}$ requires roughly twice the computational work as for two resonance structures, since there are two unique off-diagonal matrix elements to be evaluated, $\langle T_1|\hat{H}|T_2\rangle$ and $\langle T_1|\hat{H}|T_3\rangle$. As with the singlet, the shapes of φ_a, φ_b, φ_c, and φ_d are transferred between subwave functions by a symmetry operation, in this case a C_2 rotation. This leads to two unique orbitals, φ_a and φ_c in (21a) just as there was one unique orbital for the GRVB singlet. We actually optimize four orbitals, the two GVB natural orbitals

$$\varphi_1 = \varphi_a + \varphi_b \tag{30a}$$

$$\varphi_2 = \varphi_a - \varphi_b \tag{30b}$$

and the two high spin orbitals φ_c and φ_d. By combining the high spin orbitals as

$$\varphi_3 = \varphi_c + \varphi_d \tag{30c}$$

$$\varphi_4 = \varphi_c - \varphi_d \tag{30d}$$

we can impose symmetry constraints on the orbitals, so that φ_1 and φ_3 are symmetric under vertical reflection plane, while φ_2 and φ_4 are antisymmetric. Thus, just as for the singlet, there are ten orbital rotations involved in calculating the triplet state.

For the antiresonant GRVB(1/2) triplet state, using two resonance structures to optimize the orbitals is not a restriction, because the first two describe the $^3E_{ux}$ state, while the third and fourth structures describe the $^3E_{uy}$ state. There is no matrix element coupling these states; hence, they cannot interact.

V. Results and Discussion—Square Geometry

In Figure 3 we show the energy levels (relative to the $^1B_{1g}$ state) resulting from a full π CI calculation, along with the HF and GRVB results. The full π CI is the fully correlated limit of this basis set (which excludes the σ sigma space) and thus represents the "correct" set of energy levels to which we can compare HF and GRVB. The disadvantage of the full CI wavefunction is that we cannot extract a simple conceptual description from the multitude of configurations, as we can from the HF and GRVB wave functions.

The GRVB results are seen to be in very good agreement with the full π CI. The ground state is correctly predicted to be $^1B_{1g}$, the first triplet is about 10 kcal higher (CI: 10.2, GRVB: 13.0), and the $^1A_{1g}$ and ^3E_u antiresonant states are at about 50 and 100 kcal, respectively. Thus, the key features of the valence state spectrum are produced by the resonating VB model. [The ionic $^1B_{2g}$ state was not calculated with GRVB or R-GVB].

The HF results are in distinctly poorer agreement with the CI. The ground state is incorrectly predicted to be a triplet (a relative error of 14.6 kcal), the $^1B_{2g}$ ionic state is 31.0 kcal too low, the ^3E_u state is 31.3 kcal too high, and the $^1A_{1g}$ and $^1B_{2g}$ states are interchanged.

In Figure 4 we show one bond pair from the GVB(2/4) singlet wave function [(16)]. The orbitals are seen to be strongly localized and polarized to achieve favorable bonding overlaps. The GRVB(2/4) orbitals from the resonant ($^1B_{1g}$) and antiresonant ($^1A_{1g}$) states are also displayed and are virtually indistinguishable from the GVB orbitals. In contrast to benzene, for example, the orbitals are completely localized even before resonance is included. This is discussed in the next section.

Figure 5 shows the orbitals for the lowest triplet states [from the nonresonant GVB(1/2) and resonant and antiresonant triplet GRVB(1/2) wave functions]. In contrast to the singlet state, the triplet orbitals are completely delocalized in the GVB wave function and become very localized in the GRVB wave functions. At the GVB level, the orbitals try to include the effect of resonance by smearing out over the molecule. This tendency is so strong that the GVB "bond pair" is distorted into a bond between the diagonal carbons! When the resonance is explicitly included in the two-structure GRVB wave function, the orbitals are free to

(16) φ_a is allowed to overlap φ_b, of course, because they are singlet-paired.

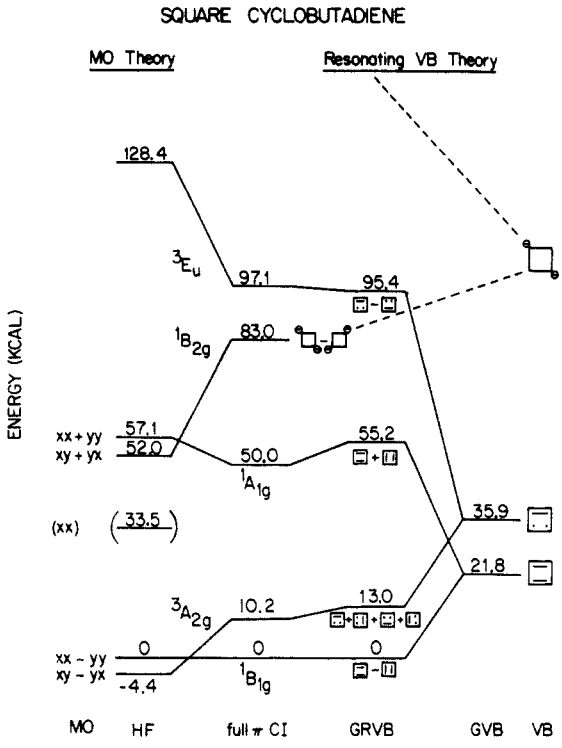

Figure 3. Quantitative comparison of MO theory and resonating VB theory. The total energies for the $^1B_{1g}$ state are the following: HF, −153.58584; GRVB, −153.65295; and full π CI, −153.65783. The GRVB and π CI wave functions use the same frozen σ core, while the core orbitals for the HF wave functions are completely relaxed for each state.

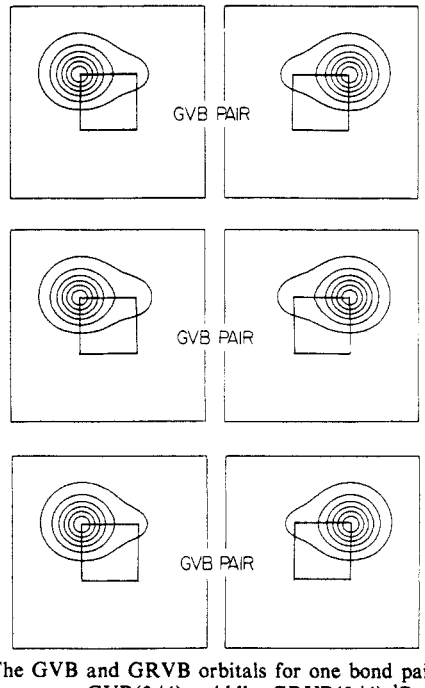

Figure 4. The GVB and GRVB orbitals for one bond pair of singlet cyclobutadiene: top, GVB(2/4); middle, GRVB(2/4) $^1B_{1g}$ (resonant) state; bottom, GRVB(2/4) $^1A_{1g}$ (antiresonant) state. Only one of the two (equivalent) bond pairs is shown in each case. All orbitals are plotted in a plane to 0.5 Å above, and parallel to, the plane of the molecule. The projected positions of the atoms are included on the plots for clarity, and the contours range from −1.0 to 1.0 au by increments of 0.05, with negative contours represented by dotted lines.

localize and take on shapes expected from VB theory. This occurs in most systems to which we have applied GRVB, and the next section discusses why the CBD singlet state is an exception. Another noticeable feature of the GRVB triplet orbitals is that the antiresonant state orbitals are more localized than those of the resonant state. The "tightening up" of each orbital reduces

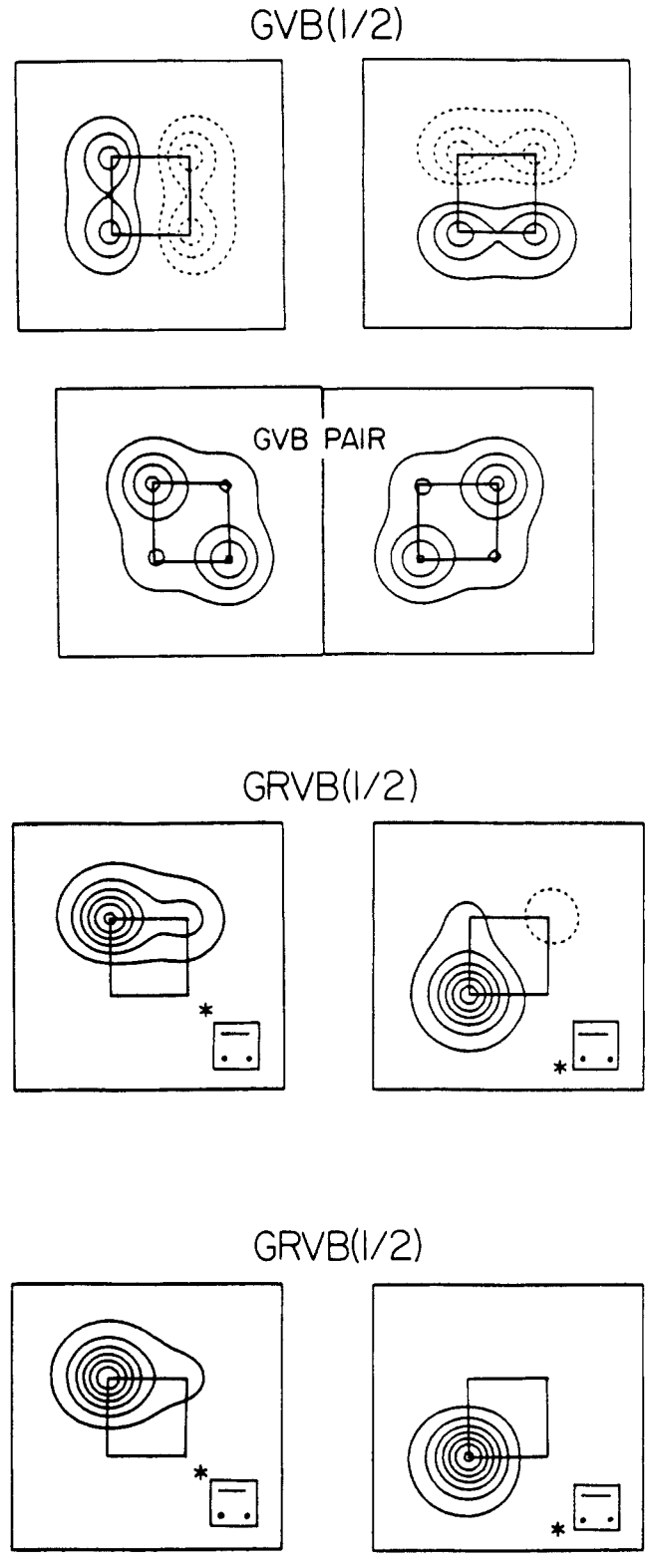

Figure 5. The GVB and GRVB orbitals for triplet cyclobutadiene: top, GVB(1/2) (nonresonant); middle, GRVB(1/2) $^3A_{2g}$ (resonant) state; bottom, GRVB(1/2) ^3E_u (antiresonant) state. The asterisk indicates which GVB orbital is being plotted.

the interaction between the two resonance structures, thereby reducing the amount that the antirresonant state is driven up in energy from the energy of a single resonance structure. It is important to understand that reducing this "interaction" does not necessarily mean reducing the wave function overlap. In optimizing the antiresonant wave function it is the whole energy term

$$E_{ANTI} = H_{AA} - \frac{H_{AB} - S_{AB}H_{AA}}{1 - S_{AB}} \qquad (31)$$

that must be minimized (here H_{AA} and H_{AB} are the digonal and off-diagonal Hamiltonian matrix elements); however, the wave function overlap (S_{AB}) does indeed decrease from 0.0826 for the resonant state to 0.00323 for the antiresonant state.

It is interesting that the "ionic" $^1B_{2g}$ state is actually below the antiresonant triplet state. Perhaps a better description of the $^1B_{2g}$ state is as a resonance of two structures, each of which has four one-electron bonds. By appropriately singlet-coupling pairs of these one-electron bonds, we obtain the desired $^1B_{2g}$ symmetry

$\psi^{R\text{-}VB}(^1B_{2g}) =$ 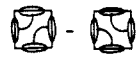 (32)

Since the carbon–carbon two-electron π bond is more than twice as strong as the one-electron π bond, the four one-electron bonds will not be competitive with two two-electron bonds. However, it seems reasonable that such a structure might be more stable than the structure with two electrons in a single p orbital (24). The antiresonant combination of these "ionic" structures leads to a state with A_{1g} symmetry, and thus the $^1A_{1g}$ state at 50.0 kcal may contain a small amount of this character. This would explain why the GRVB description of the $^1A_{1g}$ state is 5.2 kcal too high, since the GRVB wave function does not include this "ionic character".

Finally, we note that the GRVB value for the $^1B_{1g}$ to $^3A_{2g}$ excitation is 2.8 kcal *above* the CI value. Since the correlation error in the two bond pairs should be greater than the correlation error in one bond pair plus a triplet-coupled pair, this result is opposite to expectation. One possible explanation is that the triplet resonance is not completely described, a result of using only two resonance structures to optimize the orbitals. As discussed in section IV, we believe this error is negligible. Another possibility is that the $^3A_{2g}$ state requires contributions from the one-electron bond structures

$\psi(^3A_{2g}) =$ 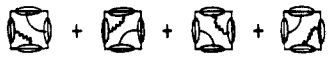 (33)

(where the wiggly line represents triplet coupling), which is included in the CI but not in the GRVB wave function.

That MO theory predicts the incorrect ground state is significant, as this is considered to represent a violation of Hund's rule.[7] Kollmar and Staemmler have proposed a mechanism they call "dynamic spin polarization"[17] by which the singlet state in a biradical species is expected to be lowered by CI more than the triplet. They have used this mechanism to justify the Hund's rule violation in H_4, twisted ethylene, and planar methane as well as in cyclobutadiene. The effect is expected to cause a state crossing when the singlet and triplet states are nearly degenerate, as occurs when the exchange integral between the two singly-occupied orthogonal orbitals is small. As discussed in section II, the exchange integral in this case is 2.2 kcal (11). The spin polarization theory is a formalized version of a qualitative explanation put forth earlier by Borden[18] to explain the cyclobutadiene violation. Without going into the details of the dynamic spin polarization theory, we simply point out that the CI terms that cause this "spin polarization" are similar to those required to convert the HF wave function into a resonating VB wave function. Thus the *"dynamic spin correlation" effect is merely the static spin-pairing of bond orbitals implicit in resonating VB wave functions.* Using the resonating valence bond model also leads to the correct ground state of square H_4, which is isomorphic to the π space of cyclobutadiene. The singlet–triplet inversion in twisted ethylene can also be explained by using a single-particle wave function[19] (spin-optimized GVB), rather than resorting to dynamic spin polarization.

VI. The VB Singlet Slate—A "Forbidden Reaction"

In the last section we saw that the GRVB(1/2) singlet orbitals differ only slightly from the GVB(2/4) orbitals. In contrast, the triplet-state orbitals are very delocalized in the GVB wave function (because they are trying to include resonance) but very localized at the GRVB level (because the resonance is included explicitly), a behavior typical of GVB and GRVB wave functions of resonating systems. The reason for this anomalous behavior of the singlet state can be understood on the basis of the orbital phase continuity principle (OPCP),[20] which is used to predict whether a reaction is "allowed" or "forbidden". The OPCP approach makes identical predictions as the Woodward–Hoffman rules[21] for systems with symmetry, but OPCP does not require symmetry to work. For example, using OPCP, the $H_2 + D_2 \rightarrow 2HD$ reaction is predicted to be forbidden for any approach geometry, because of what necessarily happens to the phases of the orbitals as they convert from the reactant bonding structure to the product bonding structure. Because the relative phases of the two orbitals in one of the bond pairs must change sign, the transition state corresponds to breaking a bond. We do not give a derivation of OPCP here, but simply state the consequence that bears on the problem at hand. *If the interconversion of two bonding structures is "allowed" by OPCP, then a Hartree-Fock or GVB-PP wave function describing one of these bonding structures may delocalize to incorporate some character from the other bonding structure. If the interconversion of the two bonding structures is OPCP "forbidden", then a Hartree–Fock or GVB-PP wave function will not delocalize to include character from the other bonding structure.* Since the π space of the cyclobutadiene singlet is isomorphic with a "forbidden" 2 + 2 reaction, the two VB structures *cannot* interconvert. Thus, the "smearing out", which allows some resonance at the GVB level, is forbidden by OPCP for the CBD singlet. To whatever extent the wave function tries to include resonance by smearing out, it picks up character of a broken bond, which is energetically unfavorable. However, this noninterconversion of bonding structures has no bearing on the amount of energy lowering that will result from resonating the two structures, and indeed the resonance energy for CBD is 22 kcal. The CBD triplet and most of the other resonating systems we have studied are isomorphic with "allowed" reactions and thus show considerable delocalization at the HF and GVB-PP levels.

An important ramification of this property of the CBD singlet is that the GRVB wave function is only slightly different than the R-GVB wave function, as shown in Figure 6. The resonance lowering for the R-GVB wave function is 20.6 kcal, only 1.2 kcal less than GRVB. Similarly, the antiresonant state only drops by 0.7 kcal in going from R-GVB to GRVB. Thus for singlet CBD, and any other resonating system that is isomorphic with a forbidden reaction, the much simpler R-GVB wave function can be

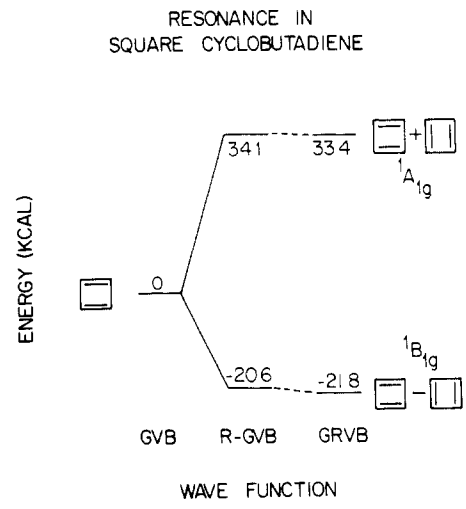

Figure 6. Resonance in cyclobutadiene from GVB(2/4), R-GVB(2/4), and GRVB(2/4) wave functions. All calculations used the same σ space.

(17) Kollmar, H.; Staemmler, V. *Theor. Chim. Acta (Berlin)* **1978**, *48*, 223. Kollmar, H.; Staemmler, V. *J. Am. Chem. Soc.* **1977**, *99*, 3583.
(18) Borden, W. T. *J. Am. Chem. Soc.* **1975**, *97*, 5968.
(19) Voter, A. F.; Goodgame, M. M.; Goddard, W. A., III *Chem. Phys.* **1985**, *98*, 7.
(20) Goddard, W. A., III *J. Am. Chem. Soc.* **1972**, *94*, 793.
(21) Hoffmann, R.; Woodward, R. B. *J. Am. Chem. Soc.* **1965**, *87*, 2046, 4388, 4389. Woodward, R. B.; Hoffmann, R. *Ibid.* **1965**, *87*, 395, 2511. Hoffman, R.; Woodward, R. B. *Angew. Chem., Int. Ed. Engl.* **1969**, *8*, 781.

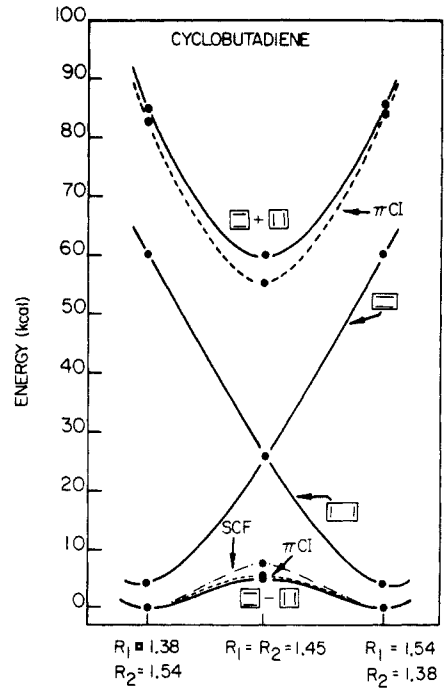

Figure 7. Resonating VB description for the rectangular distortion of square cyclobutadiene. The solid lines are R-GVB results, while the full π CI is indicated by a dashed line. Energies are with respect to the rectangular ground state.

used to obtain near-GRVB results.

Another consequence of this result is that cyclobutadiene is one of the few systems in which the electronic resonance energy can be estimated to high accuracy, because the GVB wave function corresponds very closely to the nonresonating reference state. Assuming that the resonance lowering would not change significantly upon increasing the basis set,[22] we can state that the electronic resonance energy in square cyclobutadiene is between 21.8 kcal [E(GVB) − E(GRVB)] and 23.1 kcal [$E(\Psi_A^{GRVB})$ − E(GRVB)]. [In systems where delocalization occurs at the GVB-PP level, $E(\psi_A^{GRVB})$ is usually much higher than E(GVB).]

VII. Rectangular Distortion

We now allow square CBD to distort. Based on the VB description, one expects the rectangular geometry to be the favored distortion. In resonating VB theory, there are two VB structures which are inequivalent

$$\Psi_{TOT} = C_A \boxed{} + C_B \boxed{} \qquad (34)$$

The good structure (Ψ_A) goes down in energy because it attains bond lengths closer to the ideal values for single and double bonds. The bad structure (Ψ_B) goes up in energy, leading to a decrease in the resonance energy. Thus, the molecule will distort if the good structure drops in energy faster than the resonance energy declines. Figure 7 shows the potential curves before and after resonance. The resonance is not strong enough to prevent the distortion, and the rectangular geometry is calculated to lie 4.8 kcal below square. This is in excellent agreement with the π CI result of 5.1 kcal for the same geometries.

The MO theory analysis of the distortion of square CBD relies on the second-order Jahn-Teller effect.[23] As by Pearson,[24] if a low-lying electronic state (Ψ_e) has the symmetry such that the integral $\langle\Psi_o|\partial H/\partial Q|\Psi_e\rangle$ is nonzero, then a distortion *might* occur along coordinate Q. (The integral is nonzero if the direct product of the symmetry representations of Q and Ψ_e contains the symmetry representation of the ground state Ψ_o.) The lowest MO singlet has $^1B_{1g}$ symmetry, and the first excited state has $^1B_{2g}$ symmetry. Thus a vibration with a_{2g} symmetry might cause a distortion to a nonplanar C_{4v} geometry (all hydrogens down), but such a distortion does not lower the energy. The second excited MO state has $^1A_{1g}$ symmetry which can mix into $^1B_{1g}$ via b_{1g} vibrations (rectangular distortions). In fact, this distortion does lower the energy. The HF results are also displayed in Figure 7, and HF is seen to correctly predict the ground state of the molecule to be a rectangular singlet, with an energy 7.5 kcal lower than the square singlet (and 3.1 kcal lower than square triplet).

Other theoretical estimates have been made for the rectangular stabilzation energy. Using π-electron CI calculations, Borden, Davidson, and Hart[5] obtained 4.2 kcal by using an STO-3G basis and 4.0 kcal with a double-ζ basis, while Jafri and Newton[6] obtained 6.1 kcal with a 6-31G* basis. In both these studies, the inclusion of σ correlation in the CI roughly doubled the rectangular stabilization to 8.3 kcal in the STO-3G basis[5] and 12 kcal in the 6-31G* basis.[6] Thus, the GRVB estimate presented here, which did not include σ correlation, may be too low. Whitman and Carpenter have recently put an experimental *lower bound* of 1.6 kcal on this barrier to interconversion of the rectangles, by comparing the rate of interconversion to the rate of Diels–Alder trapping.[3] The CBD was isotopically labeled in a way that yielded different trapping products for the two rectangular forms, and the activation energy for automerization was determined to be 1.6 kcal higher than the activation for trapping. Since the trapping reaction should not have a negative activation energy, 1.6 kcal is a lower bound on the CBD automerization barrier.

VIII. Conclusions

We have applied MO theory and resonating VB theory to understand the low-lying states of cyclobutadiene in its square geometry. The MO description casts CBD as a diradical with a triplet ground state and a corresponding open shell singlet slightly higher. In contrast, VB theory describes ground state CBD as a resonance of two structures, each with two π bonds; here the triplet state is higher because it has one broken bond. Through the use of HF and GRVB techniques, the orbital-optimized versions of the MO and resonating VB wave functions can be found, and the resulting state energies are consistent with the model predictions. Comparison to the results of a full π CI indicates that *the VB model more accurately portrays the features of the CBD system, giving the correct ground state and reasonable excitation energies.* The VB approach thus provides a simple explanation of why the ground state is a singlet.

While in MO theory CBD is often described as "antiaromatic" and attributed with a negative resonance energy,[25] we find a *positive resonance energy* of 22 kcal with respect to a single VB structure. This apparent discrepancy results from a difference in the conventions for the reference energy. In MO theory, polyenes are taken to have zero resonance energy,[25,26] while in VB theory, individual VB structures are taken as the zero-resonance reference.

In VB theory, the distortion to a rectangular geometry is favored by a relaxation of strained bonds and disfavored by a loss of resonance energy. VB theory suggests that rectangular distortions should be the favored ones, and the calculations show that the strain relaxation dominates the resonance loss to yield a rectangular geometry. However, whether square or rectangular wins is not predicted from such qualitative arguments (calculations are required). In MO theory the distortion is possible due to a second-order Jahn-Teller coupling with the $^1A_{1g}$ state. Neither theory predicts qualitatively whether the distortion will actually occur, but the HF and GRVB calculations both find a rectangular singlet ground state, as does the full π CI.

(22) The resonance energy calculated by using R-GVB with the GVB pair coefficients relaxed changes from 28.5 kcal with a STO-3G basis to 21.7 kcal with a VDZ basis.

(23) Öpik, U.; Pryce, M. H. L. *Proc. Roy. Soc. London, A* **1957**, A238, 425.

(24) Pearson, R. G. *J. Am. Chem. Soc.* **1969**, *91*, 4947.

(25) Kollmar, H. *J. Am. Chem. Soc.* **1979**, *101*, 4832.

(26) Dewar, M. J. S. *The Molecular Orbital Theory of Organic Chemistry*; McGraw-Hill: New York, 1968.

Acknowledgment. Initial parts of this work were supported by the Department of Energy (Contract No. DE-AM03-76SF00767; Project Agreement No. DE-AT03-80ER10608), and completion of this work was under the National Science Foundation (Grant No. CHE80-17774). Early unpublished studies by Robert Walkup and Wilson Ho (Caltech Senior Thesis, 1975) which used full GVB (SOGI) calculations to obtain similar results are hereby acknowledged.

Registry No. CBD, 1120-53-2.

Hybridization and the Orientation and Alignment of π-Orbitals in Nonplanar Conjugated Organic Molecules: π-Orbital Axis Vector Analysis (POAV2)

R. C. Haddon

AT&T Bell Laboratories, Murray Hill, New Jersey 07974. *Received July 1, 1985*

Abstract: The concept of hybridization of atomic orbital basis functions to produce spatially directed wave functions with the orientation necessary for bond formation is fundamental to the modern understanding of the molecular and electronic structure of molecules. In the present article, we consider a bonding situation which has become increasingly important in recent years—nonplanar conjugated organic molecules, which are usually considered to possess formal sp^2 hybridization. It is shown that with a single assumption, it is possible to obtain analytical solutions for the hybridization in such compounds which in turn leads directly to the orientation of the π-orbital axis vectors (POAV) and hence to a measure of π-orbital alignment and overlap in distorted π-electron systems of known geometry. The π-orbital axis vector (POAV) analysis provides a vivid picture of the π-bonding in nonplanar conjugated organic molecules and the manner in which the σ-system has rehybridized and adjusted to facilitate the maintenance of favorable π-orbital overlap. The method is nonparametric and merely requires the atomic coordinates of the molecule or molecular fragment for its implementation (computer program POAV2 has been deposited with the Quantum Chemistry Program Exchange). The analysis is based on the sp hybrid orthogonality relationships and the geometry of the σ-skeleton. As such the method provides the most logical and natural bridge between the σ–π separability assumed in planar conjugated systems and the realistics of π-bonding in nonplanar situations. The analysis is not recommended in circumstances where the σ-bond angles are less than 100°, but with this proviso the method may be used with confidence. The general practice of quoting formal dihedral angles as a measure of π-orbital alignment or strain is strongly discouraged—such an approach is misleading, arbitrary, and equivocal. The POAV analysis has been used to provide insight into the electronic structure of a number of nonplanar conjugated organic systems of topical interest.

The concept of hybridization of atomic orbital basis functions to produce spatially directed wave functions with the orientation necessary for bond formation[1] is fundamental to the modern understanding of the molecular and electronic structure of molecules.[2-4] In general, however, it is not possible to assign hybridization (sp) from a consideration of molecular structure (or vice versa) in organic compounds of low symmetry (see below). In these cases, an energy calculation must be carried out to optimize the atomic orbital coefficients and the resulting wave function analyzed to provide an indirect index of the hybridization.[5-9] The maximum overlap method (MOM)[10] is a particularly successful variant of this approach in which the atomic hybridizations within the molecule are adjusted to maximize the total overlap of all bonds (suitably weighted by the empirical bond energies).

In the present article, we consider a bonding situation which has become increasingly important in recent years—nonplanar conjugated organic molecules,[11-13] which are usually considered to possess formal sp^2 hybridization. It is shown below that with a single assumption, it is possible to obtain analytical solutions for the hybridization in such compounds which in turn leads directly to the orientation of the π-orbital axis vectors (POAV) and hence to a measure of π-orbital alignment and overlap in distorted π-electron systems of known geometry.

In order to carry through this treatment, it is necessary to assume that the σ-bonds lie along the internuclear axes of the molecule. Thus the POAV model depends for its validity on the idea that the primary dislocations in bonding will occur among the π-electrons. In the main, this will take the form of torsional distortions, the energy of which is very much less than the energies required to bend σ-bonds in most situations. As shown below, it is quite evident that the more flexible σ-systems of many nonplanar conjugated organic molecules do much to accommodate the conformational preferences of the π-system, and this is re-

(1) Pauling, L. *J. Am. Chem. Soc.* **1931**, *53*, 1367.
(2) Pauling, L. *Nature of the Chemical Bond*; Cornell University: Ithaca, NY, 1960.
(3) Mislow, K. *Introduction to Stereochemistry*; Benjamin: New York, 1966.
(4) McWeeny, R. *Coulson's Valence*, Oxford University: London, 1979.
(5) Hunt, W. J.; Hay, P. J.; Goddard, W. A., III *J. Chem. Phys.* **1972**, *57*, 738.
(6) Chipman, D. M.; Kirtman, B.; Palke, W. E. *J. Am. Chem. Soc.* **1976**, *65*, 2256.
(7) Palke, W. E. *Croat. Chem. Acta* **1984**, *57*, 779.
(8) Foster, J. M.; Boys, S. F. *Rev. Mod. Phys.* **1960**, *32*, 300. Boys, S. F. *Rev. Mod. Phys.* **1960**, *32*, 306.
(9) Edmiston, C.; Reudenberg, K. *Rev. Mod. Phys.* **1963**, *35*, 457.
(10) Randic, M.; Maksic, Z. B. *Chem. Rev.* **1972**, *72*, 43.
(11) Greenberg, A.; Liebman, J. F. *Strained Organic Molecules*; Academic: New York, 1978.
(12) Watson, W. H., Ed. *Stereochemistry and Reactivity of Systems Containing π-Electrons*; Verlag Chemie: Miami, FL, 1983.
(13) Nakazaki, M.; Yamamoto, K.; Naemura, K. *Top. Curr. Chem.* **1984**, *125*, 1.

0002-7863/86/1508-2837$01.50/0